Journal of Plant Interactions

ISSN: 1742-9145 (Print) 1742-9153 (Online) Journal homepage: https://www.tandfonline.com/loi/tjpi20

Leaf tensity: a method for rapid determination of water requirement information in *Brassica napus* L.

Deke Xing, Xiaojian Xu, Yanyou Wu, Yujing Liu, Yansheng Wu, Jiheng Ni & Ahmad Azeem

To cite this article: Deke Xing, Xiaojian Xu, Yanyou Wu, Yujing Liu, Yansheng Wu, Jiheng Ni & Ahmad Azeem (2018) Leaf tensity: a method for rapid determination of water requirement information in *Brassica napus* L., Journal of Plant Interactions, 13:1, 380-387, DOI: 10.1080/17429145.2018.1478006

To link to this article: https://doi.org/10.1080/17429145.2018.1478006

Published online: 11 Jun 2018.

JOURNAL OF PLANT INTERACTIONS
2018, VOL. 13, NO. 1, 380–387
https://doi.org/10.1080/17429145.2018.1478006

Taylor & Francis
Taylor & Francis Group

RESEARCH ARTICLE

OPEN ACCESS Check for updates

Leaf tensity: a method for rapid determination of water requirement information in *Brassica napus* L.

Deke Xing [a], Xiaojian Xu[a], Yanyou Wu[b], Yujing Liu[a], Yansheng Wu[a], Jiheng Ni[a] and Ahmad Azeem[a]

[a]Key Laboratory of Modern Agricultural Equipment and Technology, Ministry of Education, Institute of Agricultural Engineering, Jiangsu University, Zhenjiang, People's Republic of China; [b]Research center for Environmental Bio-Science and Technology, State Key Laboratory of Environmental Geochemistry, Institute of Geochemistry, Chinese Academy of Sciences, Guiyang, People's Republic of China

ABSTRACT

Water regulation caused by enzymes, such as carbonic anhydrase (CA), changes the water status, making it difficult to diagnose water deficit using leaf water potential (ψ_L) or stomatal conductance (g_s). Therefore, new methods for timely and accurately determining plant water status should be established. In this study, CA activity, ψ_L, leaf tensity (T_d), photosynthetic characteristics and plant growth of *Brassica napus* L. seedlings under drought and subsequent rewatering were analysed. Results indicated that T_d could reflect the plant water status better than ψ_L or g_s and played an important role in the photosynthesis of *B. napus*. *B. napus* exhibited good restorability at the 40 g L^{-1} polyethylene glycol level. The rewatering strategy for *B. napus* was excellent at 40 g L^{-1} (−0.15 MPa) →20 g L^{-1} (−0.11 MPa). T_d could be used for the rapid determination of water requirement information in *B. napus* during winter drought period.

ARTICLE HISTORY
Received 27 January 2018
Accepted 14 May 2018

KEYWORDS
Carbonic anhydrase; irrigation time; photosynthetic characteristics; plant dry weight; water potential

1. Introduction

Rape is an important oil crop in China and other countries. This crop is mainly planted in southern China and used as a material for edible oil extraction or feedstock for fuel extraction, offering great economic values (Bhardwaj et al. 2015). In the karst regions of southwestern China, the hot and humid climate and widely developed karst environment are conducive for the formation of loam, which can be used to cultivate plants. For example, the soil used for cultivation in Puding County, Guizhou Province, is mainly loam (Wang et al. 2010). However, the plants in these regions usually suffer from frequent temporary water deficiency because of a considerably shallow soil with low water-holding capacity. Moreover, the agricultural water resource in these regions is very scarce, especially during the winter drought period. As a result, crop production is low and local economic development is impeded (Zhu 1997). *Brassica napus* L., a commonly cultivated type of rape, is characterized by high grain yield and is therefore suitable for widespread cultivation in the karst regions (Qaderi et al. 2007). In addition, correct timing of *B. napus* irrigation helps to reduce agricultural irrigation costs and ensure good crop yield.

Carbonic anhydrase (CA, EC 4.2.1.1) are zinc-containing metalloenzymes that catalyze the reversible conversion of CO_2 to bicarbonate. CA are widely distributed and involved in diverse physiological processes in animals, plants, archaea and eubacteria (Hu et al. 2011). Under drought stress conditions, CA activity in plants is activated. CA then catalyses the conversion of intracellular bicarbonate into H_2O and CO_2, changes cell water status and delays the water requirement in plants (Fernández et al. 2015). The instantaneous indicators, such as leaf wilting degree, predawn leaf water potential (ψ_L), stem water potential, stomatal conductance (g_s), transpiration rate (E), leaf water content (WC) and stem diameter, are traditionally considered as the indirect indexes for determining water status in plant (Gallardo et al. 2006; Zhang et al. 2011; Pathan et al. 2014; Gaudin et al. 2017; Milliron et al. 2018). However, water regulation caused by enzymes, such as CA in plants, changes the water status and volume of cells, making it difficult to diagnose water deficit using ψ_L, g_s or other indirect indexes. Therefore, new methods or indicators for timely and accurately determining plant water deficit status and physiological drought resistance should be established to predict the appropriate irrigation time.

Water status is significantly related to cell turgidity or shrinkage in plant leaves, which are composed of numerous cells. The variation of cell volume is caused by cell turgidity or shrinkage (Turner and Burch 1983). Variations in cell volume and cell sap concentration are indicated by leaf tensity (T_d). The physiological capacitance (C_P) and ψ_L are related to the cell sap concentration. Leaf C_P is associated with the effective thickness (d) and area (A) of leaves in contact with capacitor plates. The ratio of A and d is defined as leaf tensity ($T_d = A/d$) (Zhang et al. 2015). Furthermore, T_d exhibits a better relationship with net photosynthetic rate than ψ_L; therefore, changes in T_d can reflect the leaf water status (Turner and Burch 1983; Irigoyen et al. 1992; Wu et al. 2015). Photosynthetic activity is always inhibited when plants suffered from drought stress (Batra et al. 2014), which causes serious yield and economic losses (Kleiber et al. 2017). The rapid and accurate prediction of photosynthesis provides methods for determining the physiological drought resistance threshold. Irrigation based on this threshold may prevent the excessive decline of crop yield. However, studies have found indirect relationships between photosynthesis and water status and obtained results based on the irreversible damages

CONTACT Deke Xing xingdeke@ujs.edu.cn; Yanyou Wu wuyanyou@mail.gyig.ac.cn

found in the plants (Xing and Wu 2012; Wu et al. 2016; Kleiber et al. 2017). Thus, direct relationships between photosynthesis and T_d combined with the latter's rapid determination can help to quickly determine the physiological drought resistance threshold and predict the appropriate irrigation time.

In this study, *B. napus* was selected as the experimental material. The effects of drought and subsequent rewatering on CA activity, ψ_L, C_P, photosynthetic traits, leaf area (A) and plant dry weight of seedlings were analysed. Variations in T_d and water requirement information in *B. napus* were also investigated. The irrigation time of *B. napus* was then determined. The results could provide a new method for rapidly determining the appropriate irrigation time of *B. napus* during winter drought period using T_d.

2. Materials and methods

2.1. Plant growth and treatment

The new hybrid rapeseed Qianyou No. 17 was used. It exhibits high yield, strong resistance and good quality in *B. napus* commonly planted in the karst area of southwest China. The seedlings and plants of *B. napus* were germinated, cultivated and treated according to Xing et al. (2016) in a growth chamber at the Institute of Agricultural Engineering, Jiangsu University, Jiangsu Province, China (32.20° N, 119.45° E). The *B. napus* plants were sown in 12-hole trays containing quartz sand and grown in a growth chamber with 12 h photoperiods [300 μmol m^{-2} s^{-1} Photosynthetic Photon Flux Density (PPFD)], day/night temperatures of 28°C/20°C and relative air moisture level of 70%. After 2 months of growth, four drought stress levels were created by preparing 4 concentrations of poly-ethylene glycol (PEG) 6000 (i.e. 0, 20, 40 and 80 g L^{-1}) with corresponding water potentials of −0.08, −0.11, −0.15 and −0.22 MPa (Michel and Kaufmann 1973). Rewatering was conducted on day 8 from the onset of the drought stress treatment. The seedlings, which grew in 0, 20, 40 and 80 g L^{-1} PEG treatment solutions, were transferred into 0, 10, 20 and 40 g L^{-1} PEG treatment solutions with corresponding −0.08, −0.09, −0.11 and −0.15 MPa water potentials, respectively. The rewatering phase lasted for 4 days. The solution was changed with a new batch of mixed solution every other day during the treatments. The fourth and fifth youngest fully expanded leaves from the top (three plants from each treatment group) were chosen for measurement. Determination was conducted on day 8 from the onset of the drought stress treatment and on day 4 from the onset of the rewatering treatment.

2.2. Determination of CA activity, photosynthesis and chlorophyll-a fluorescence parameters

The fourth and fifth youngest fully expanded leaves from the top were chosen for CA activity measurement. Three plants from each treatment group were used for the measurement. Leaf tissues (0.3–0.8 g) were quickly frozen in liquid nitrogen and ground with 3 mL extraction buffer (0.01 mol L^{-1} barbitone sodium with 0.05 mol L^{-1} mercaptoethanol, pH 8.3). The homogenate was centrifuged at 13,000 r min^{-1} and 0°C for 5 min and then placed on ice for 20 min. CA activity was determined with the electrometrical method of Wilbur and Anderson (1948) with modifications (Xing and Wu 2012). In brief, CA activity was assayed at 0–2 °C in a mixture containing 4.5 mL 0.02 mol L^{-1} barbitone buffer (5, 5-diethylbarbituric acid; pH 8.3), 0.4 mL sample and 3 mL CO_2-saturated water. CA activity was expressed in Wilbur and Anderson (WA) units as $WA = (t_0/t) - 1$, where t_0 and t were the time (second) measured for the pH change (8.2–7.2) with buffer alone (t_0) and with sample (t).

The net CO_2 assimilation rate (A_n, μmol (CO_2) m^{-2} s^{-1}) and stomatal conductance (g_s, mol m^{-2} s^{-1}) were measured with the method described by Xing and Wu (2012). Chlorophyll-*a* fluorescence (ChlF) was measured with a pulse amplitude modulated ChlF imaging system (*IMAGING-PAM, Heinz Walz GmbH*, Effeltrich, Germany). Before the measurements, the leaves were dark-adapted for 30 min to ensure complete relaxation of all reaction centers. The minimum chlorophyll fluorescence (F_o) was determined using a measuring beam, whereas the maximum chlorophyll fluorescence (F_m) was recorded after a 0.8 s saturating light pulse (6000 μmol m^{-2} s^{-1}). The maximum quantum yield of photosystem II (F_v/F_m) was calculated using the following equation: $F_v/F_m = (F_m - F_o)/F_m$.

2.3. Determination of leaf water content, water potential, physiological capacitance and leaf tensity

The leaf was dried in an oven at 80°C. The fresh and dry weights were measured using an electronic analytical balance (*BSA124S, Sartorius*, Gottingen, Germany), and WC was calculated according to the difference between the fresh and dry weights of leaf. C_P was measured using an LCR tester (model 3532-50, Hioki, Nagano, Japan) with a frequency and voltage of 3 kHz and 1 V, respectively. The leaf was clipped in a custom-made parallel-plate capacitor (Zhang et al. 2015). Using a dew point microvoltmeter in a universal sample room (C-52-SF, Psypro, Wescor, Logan, Utah), ψ_L was measured at the same position of the leaves with C_P testing. Moreover, T_d was calculated according to Equation (1).

$$T_d = \frac{A}{d} = \frac{C_P}{\varepsilon_0}\left[\frac{1000iRT}{81000iRT + (81 - a)M\Psi_L}\right] \quad (1)$$

where A is the effective area of the leaf in contact with the capacitor plates expressed in cm^2, d is the leaf effective thickness expressed in cm, i is the dissociation coefficient with a value of 1, R is the gas constant with a value of 0.0083 L MPa mol^{-1} K^{-1}, T is the thermodynamic temperature ($T = 273 + t$°C) expressed in K, ε_0 is the vacuum dielectric constant with a value of 8.854×10^{-12} F m^{-1}, a is the relative dielectric constant of cytosol solute, M is the relative molecular mass of the cytosol solute expressed in g mol^{-1}, and the value 81 is the relative dielectric constant of water at normal temperature. In this study, the sugar $C_{12}H_{22}O_{11}$ was identified as the solute in the cytosol; therefore, a was 3.3, M was 342 g mol^{-1}, and the temperature was 20°C. Equation 1 could be rewritten as follows:

$$T_d = \frac{C_P}{(717.17 + 96.75\Psi_L)} \quad (2)$$

2.4. Mathematical model between net CO_2 assimilation rate and leaf tensity

The A_n – C_i response curves are fitted using the following equation:

$$A_n = \frac{CE \times C_i \times A_{\max}}{CE \times C_i + A_{\max}} - R_{\text{esp}} \quad (3)$$

where A_n is the net CO_2 assimilation rate [μmol (CO_2) m^{-2} s^{-1}], CE is the carboxylation efficiency [μmol (CO_2) m^{-2} s^{-1}], C_i is the intracellular CO_2 concentration (μmol mol^{-1}), $A_{\max}$ is the net CO_2 assimilation rate at CO_2 saturation [μmol (CO_2) m^{-2} s^{-1}], and R_{esp} is the photorespiration rate [μmol (CO_2) m^{-2} s^{-1}].

Incorporating $a = A_{\max}$, $b = A_{\max}/CE$ and $Y_0 = -R_{\text{esp}}$ into Equation 3, we can obtain the following expression:

$$Y = Y_0 + \frac{aX}{b + X} \quad (4)$$

where Y is defined as the net H_2O assimilation rate [μmol (H_2O) m^{-2} s^{-1}], X is the leaf tensity (T_d, cm), $-Y_0$ is the physiological water loss rate [i.e. transpiration and guttation, μmol (H_2O) m^{-2} s^{-1}]; a is the net H_2O assimilation rate when the intracellular water is sufficient [μmol (H_2O) m^{-2} s^{-1}], and a/b is the hydration efficiency expressed as UT m^{-3} s^{-1}, where UT is equal to 10^2 μmol.

CO_2 and H_2O are both substrates for photosynthesis, and the net assimilation rate for H_2O is similar to that for CO_2. Moreover, the plant leaf is composed of a large number of cells, and the variation of cell sap concentration and cell volume can be reflected by T_d, which can indicate plant water status. Therefore, the relationship between A_n and T_d can also be fitted using Equation (4).

2.5. Measurement of chlorophyll content, leaf area and plant dry weight

The chlorophyll content (SPAD) was measured using a chlorophyll meter (*SPAD-502, Konica Minolta*, Tokyo, Japan). Leaf area (A) was measured using a portable leaf area meter (*AM-200, ADC*, UK), from the onset of the drought stress treatment to day 18. Five plants from each treatment group were selected and dried in an oven at 80° C at the end of the drought and subsequent rewatering treatments. Dry weight per plant (g) was measured using an electronic analytical balance (*BSA124S, Sartorius*, Gottingen, Germany).

2.6. Leaf area growth model

Given that the growth rate of A can reflect the plant growth status, the relationship between A and time (D) can be fitted using a four – parameter logistic equation (Equation 5).

$$A = A_0 + \frac{a}{1 + (D/D_0)^b} \quad (5)$$

where A_0 is the initial leaf area during logarithmic growth phase, a is the upper limit of the leaf area, D_0 is the number of days when the leaf area reaches half of the maximum value during the logarithmic growth phase, and b is a constant.

The duration from the onset of observation to the logarithmic growth phase is calculated as follows:

$$DT_s = D_0 + \frac{2D_0}{b} \quad (6)$$

The duration of the logarithmic growth phase is calculated as follows:

$$DT\log = \frac{-4D_0}{b} \quad (7)$$

Then, the relative time required when the growth rate of the leaf area reaches the maximum value (RT_{GRM}) is calculated as follows:

$$RT_{\text{GRM}} = \frac{D_0 - DT_s}{DT_{\log} + DT_s} \quad (8)$$

The lower the RT_{GRM} value, the faster the growth rate of the leaf area reaches the maximum value.

2.7. Statistical analysis

All collected data were analysed using SPSS software (version 13.0, SPSS Inc.). The differences between the drought stress levels were assessed using the least significant difference post-hoc test at 5% significance level ($P \leq 0.05$). Data were shown as the means ± standard errors determined using one-sample T test. The confidence interval was 95%.

3. Results

3.1. CA activity

During the drought phase, the CA activity at 20 and 40 g L^{-1} PEG levels was the highest (Figure 1). The CA activities at 0 and 40 g L^{-1} PEG levels were significantly reduced after rewatering compared with those in the drought phase. By comparison, the CA activity at 20 g L^{-1} PEG level increased after rewatering compared with that in the drought phase. CA activities at 20 and 40 g L^{-1} PEG levels were all higher than those at 0 g L^{-1} PEG level during drought and rewatering phases.

3.2. Leaf water content, water potential and leaf tensity

A significantly lower value of WC was observed at 80 g L^{-1} PEG level compared with that at 0 g L^{-1} PEG level during the drought phase. Moreover, significant decreases of WC values were found at 40 and 80 g L^{-1} PEG levels compared

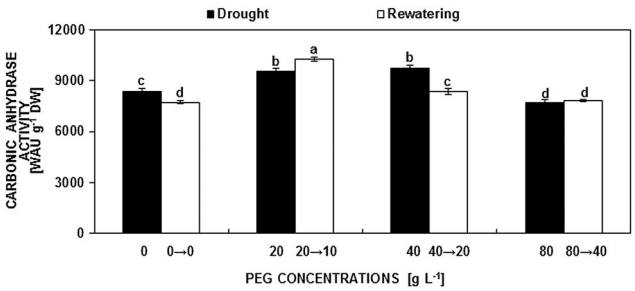

Figure 1. Effect of drought and subsequent rewatering on carbonic anhydrase activity (CA, WAU g^{-1} DW).

Note: The mean ± SE ($n = 5$) followed by different letters differ significantly at $P \leq 0.05$, according to one-way ANOVA and t test; Arrows (→) indicate that the plants were transferred from one treatment solution into another.

Table 1. Effect of drought and subsequent rewatering on leaf water content (WC, %), water potential (ψ_L, MPa) and leaf tensity (T_d, cm)[a].

Drought Phase				Rewatering Phase[b]			
PEG concentrations (g L^{-1})	WC	ψ_L	T_d	PEG concentrations (g L^{-1})	WC	ψ_L	T_d
0	88.51 a (0.04)	−0.74 a (0.04)	4.66 a (0.05)	0→0	87.01 a (0.04)	−1.18 b (0.04)	3.11 a (0.06)
20	86.34 ab (0.02)	−0.72 a (0.04)	3.89 b (0.19)	20→10	84.18 ab (0.02)	−0.75 a (0.02)	2.11 b (0.06)
40	85.66 ab (0.03)	−2.20 b (0.03)	1.77 c (0.01)	40→20	82.44 b (0.02)	−0.77 a (0.03)	1.87 c (0.10)
80	83.35 b (0.01)	−2.80 c (0.05)	1.33 d (0.01)	80→40	82.47 b (0.03)	−1.12 b (0.06)	1.55 d (0.02)

[a]Means in the same column followed by different letters differ significantly at $p \leq 0.05$, according to one-way ANOVA and *t*-test (standard errors shown in parentheses).
[b]Arrows (→) indicate that the plants were transferred from one treatment solution into another.

with that at 0 g L^{-1} PEG level during the rewatering phase (Table 1). However, the value of WC at each treatment level during the drought phase showed no significant difference compared with that during the rewatering phase. During the drought phase, ψ_L values at 40 and 80 g L^{-1} PEG levels were significantly lower than those of the other two levels. The ψ_L value at 80 g L^{-1} PEG level was the lowest, and the values at 0 and 20 g L^{-1} PEG levels showed no significant difference (Table 1). The ψ_L values at 40 and 80 g L^{-1} PEG levels increased after rewatering compared with those in the drought phase. By contrast, the values at 0 g L^{-1} PEG level decreased after rewatering. The ψ_L values at 20 and 40 g L^{-1} PEG levels were significantly higher than those of the other two levels during the rewatering phase. Low T_d values were associated with increasing drought stress (Table 1). T_d values at 0 and 20 g L^{-1} PEG levels decreased after rewatering compared with those in the drought phase. In addition, T_d values at 40 and 80 g L^{-1} PEG levels exhibited minor increase after rewatering compared with those in the drought phase.

3.3. Photosynthetic characteristics

Low A_n values were associated with increasing drought stress during the drought phase (Figure 2(A)). The A_n values at 0 and 20 g L^{-1} PEG levels showed no significant difference during the drought phase. Those at 40 and 80 g L^{-1} PEG levels during the rewatering phase exhibited no significant difference compared with those during the drought phase. The A_n values at 20, 40 and 80 g L^{-1} PEG levels were 97%, 78% and 63% of that at 0 g L^{-1} PEG level during the drought phase. Moreover, the values at 20, 40 and 80 g L^{-1} PEG levels were 82%, 84% and 65% of that at 0 g L^{-1} PEG level during the rewatering phase. During the drought phase, g_s values at 0, 20 and 40 g L^{-1} PEG levels showed no significant difference (Figure 2(B)), whereas that at 80 g L^{-1} PEG level decreased significantly. The g_s values at 20 and 40 g L^{-1} PEG levels increased after rewatering, whereas those at 0 and 80 g L^{-1} PEG levels exhibited no significant difference after rewatering compared with those in the drought phase.

F_o values showed no significant variation as drought stress increased during drought and rewatering phases (Figure 2 (C)). F_v/F_m values were independent with increasing drought stress during the drought phase, but at 20 g L^{-1} PEG level, it was significantly lower than that at 0 g L^{-1} PEG level during the rewatering phase (Figure 2(D)). Moreover, the values of F_v/F_m at each treatment level during the drought phase showed no significant difference compared with that during the rewatering phase.

3.4. Correlation of leaf tensity, water content, water potential, stomatal conductance and net CO_2 assimilation rate

The Pearson correlation coefficients for the relationship of T_d, WC, ψ_L, g_s and A_n are shown in Table 2. T_d was significantly correlated with WC, ψ_L and A_n. A_n was significantly correlated with T_d, WC, ψ_L and g_s. However, g_s exhibited no significant relationship with T_d and WC. WC showed no significant relationship with ψ_L.

3.5. Relationship between leaf tensity and net CO_2 assimilation rate

The relationship between A_n and T_d displayed a good correlation and could be fitted well by the rectangular hyperbola equation $Y = -3.91 + (17.95X/0.91 + X)$, $R^2 = 0.84$, $n = 24$, $P < 0.0001$ (Figure 3). In other words, an increase in T_d was correlated with an increase in A_n during drought and subsequent rewatering phases. Moreover, the parameters a, b and Y_0 could be estimated using Equation (2). The physiological water loss rate, net H_2O assimilation rate when the intracellular water was sufficient and hydration efficiency were 3.91 μmol (H_2O) m^{-2} s^{-1}, 17.95 μmol (H_2O) m^{-2} s^{-1} and 19.73 UT m^{-3} s^{-1}, respectively.

3.6. Chlorophyll content, leaf area and plant dry weight

The chlorophyll content at 80 g L^{-1} PEG level was higher than those at 0, 20 and 40 g L^{-1} PEG levels during drought phase (Table 3). High chlorophyll contents were associated with increasing drought stress at 0–40 g L^{-1} PEG levels during the rewatering phase. During the drought phase, the chlorophyll contents at 20, 40 and 80 g L^{-1} PEG levels showed no significant difference compared with those during the rewatering phase. Fitting curves of the relationship between A and D are shown in Figure 4, and the corresponding fitting equations are shown in Table 4. The relationship between A and D at 0, 20 and 40 g L^{-1} PEG levels displayed good correlations. However, the negative value ($a = -1.12$) of the upper limit of leaf area at 80 g L^{-1} PEG level indicated that the plant ceased growing and the leaf wilted. RT_{GRM} values of A at 0, 20 and 40 g L^{-1} PEG levels were 0.50, 0.36 and 0.33, respectively. Low values of A were associated with increasing drought stress, whereas fast growth rate for the leaf area to reach its maximum value was associated with increasing drought stress during the drought and rewatering phases. The plant dry weight at 40 g L^{-1} PEG level did not significantly differ from that at

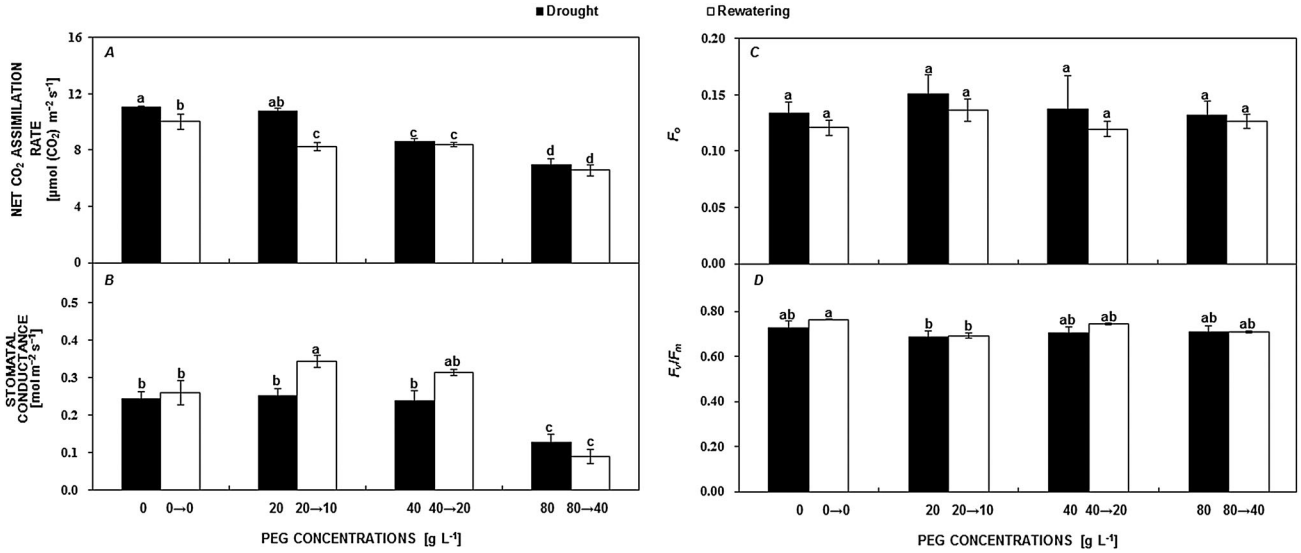

Figure 2. Effect of drought and subsequent rewatering on photosynthetic and chlorophyll-*a* fluorescence parameters (*A*, net CO_2 assimilation rate; *B*, stomatal conductance; *C*, F_o; *D*, F_v/F_m).

Note: The mean ± SE ($n = 5$) followed by different letters differ significantly at $P \leq 0.05$, according to one-way ANOVA and *t* test; Arrows (→) indicate that the plants were transferred from one treatment solution into another.

Table 2. Correlation of leaf tensity, water content, water potential, stomatal conductance and net CO_2 assimilation rate ($n = 24$).

	Water content	Water potential	Stomatal conductance	Net CO_2 assimilation rate
Leaf tensity	0.63**	0.53**	0.29	0.89**
Water content		0.14	0.33	0.58**
Water potential			0.50*	0.48*
Stomatal conductance				0.50*

**Correlation is significant at the 0.01 level (2-tailed).
*Correlation is significant at the 0.05 level (2-tailed).

0 g L^{-1} PEG level. By contrast, the plant dry weight at 80 g L^{-1} PEG level was significantly lower than that at 0 g L^{-1} PEG level (Figure 5).

4. Discussion

4.1. CA activity and leaf water status

The CA activity in *B. napus* was activated with increasing drought stress. CA then catalysed the conversion of intracellular bicarbonate into H_2O and CO_2 and altered the leaf water status under drought conditions (Wu and Xing 2012). Water regulation caused by enzymes, such as CA in plants, prevented the reduction in ψ_L at 20 g L^{-1} PEG level. The value of ψ_L was mainly influenced by vacuolar concentration (Porcel and Ruiz-Lozano 2004). The stable value of ψ_L at 20 g L^{-1} PEG level indicated that the vacuolar concentration did not vary significantly. As drought stress increased, higher CA activity at 40 g L^{-1} PEG level meant a stronger water regulation capacity, which provided more water in the cytosol of cells, and prevented the reduction of WC. The increase of g_s at 20 and 40 g L^{-1} PEG levels after the rewatering phase indicated that water deficiency in *B. napus* was prevented, and A_n demonstrated better stability at 40 g L^{-1} PEG level during the drought and subsequent rewatering phases compared with that at 20 g L^{-1} PEG level. However, the increase of vacuolar concentration and decrease of vacuole volume were still caused by increasing drought stress. As a result, T_d could respond sensitively to the drought condition. By compressing the vacuoles in cells with the reduction of T_d, water in vacuoles could then efficiently enter into the cytosol of cells, thereby improving the water supply efficiency for photosynthesis. T_d could represent the variation of water status in the cytosol, which could also be analysed according to the movement of water in the cells (Figure 6).

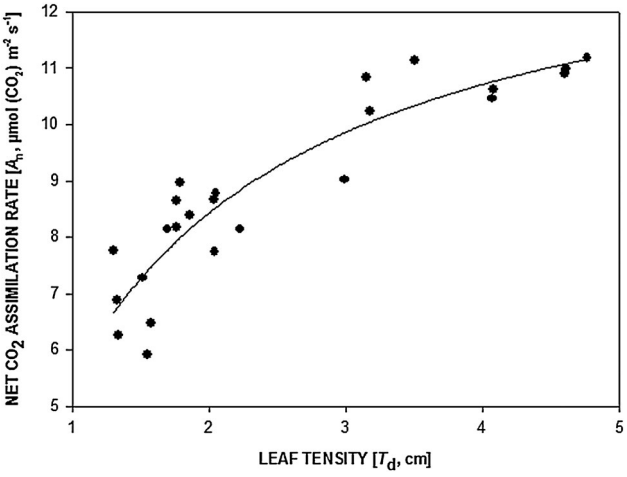

Figure 3. Fitting curves of the relationship between net photosynthetic rate [A_n, μmol (CO_2) m^{-2} s^{-1}] and leaf tensity (T_d, cm).

Furthermore, T_d exhibited good correlations with A_n, WC and ψ_L in this study. T_d could reflect the plant water status better than ψ_L or g_s and played an important role in the photosynthesis of *B. napus*.

4.2. Physiological tolerance threshold

The rectangular hyperbolic equation is derived from the Michaelis–Menten equation. The value of K in the Michaelis–Menten equation indicates the substrate concentration when the corresponding velocity is half-maximal. Similarly, the value of b in the rectangular hyperbolic equation (Equation 4) indicates the value of T_d when A_n is half-maximal (Dowd and Riggs 1965). A whole rectangular hyperbolic

Table 3. Effect of drought and subsequent rewatering on chlorophyll Content (SPAD)[a].

Drought Phase		Rewatering Phase		Increment in Chlorophyll Content During Rewatering Phase
PEG concentrations (g L^{-1})	Chlorophyll Content[a] (SPAD)	PEG concentrations[b] (g L^{-1})	Chlorophyll Content[a] (SPAD)	
0	35.93 ± 2.53 ab	0→0	38.37 ± 0.78 c	2.43
20	32.93 ± 0.73 b	20→10	44.70 ± 0.44 b	11.77
40	37.73 ± 0.99 ab	40→20	50.67 ± 2.47 a	12.93
80	39.90 ± 1.81 a	80→40	44.83 ± 2.53 ab	4.93

[a]Means ± SE. Values in the same column followed by different letters differ significantly at $p \leq 0.05$ according to one-way ANOVA and *t*-test.
[b]Arrows (→) indicate that the plants were transferred from one treatment solution into another.

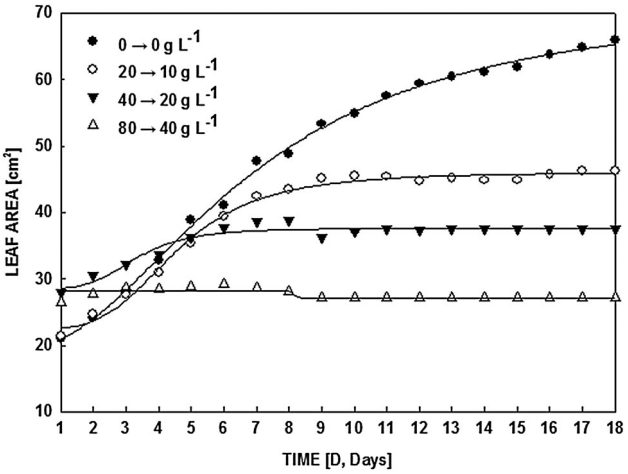

Figure 4. Fitting curves of the relationship between leaf area (A, cm^2) and time (D, Days).

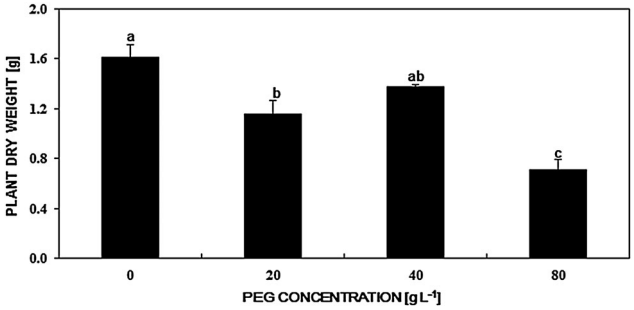

Figure 5. Effect of drought and subsequent rewatering on plant dry weight. Bars with different letters differ significantly at $p \leq 0.05$ according to one-way ANOVA and *t*-test.

curve is divided into three sections, including first-order reaction (forepart), mixed-order reaction (middle part) and zero-order reaction (back end) (Kou et al. 2005). At midpoint of the middle part ($T_d = 3b$), A_n is equal to three-quarters of the maximal value. When T_d becomes lower than 3b, A_n will be inhibited. In this study, the value of b was 0.91. When T_d was equal to 2.73 ($T_d = 3b$), the corresponding drought stress level implemented on *B. napus* was close to 40 g L^{-1} PEG level. This result indicated that the tolerance threshold of *B. napus* to drought stress was approximately 40 g L^{-1} PEG level.

Chlorophyll fluorescence parameters are widely used to indicate the tolerance of plants to environmental stresses. The photochemical apparatus of *B. napus* was not damaged under drought stress, which could be indicated by the variation of F_o. The response of F_v/F_m in *B. napus* to increasing drought stress also indicated slight damage to the PSII reaction centers under drought stress (Wu and Xing 2012). Moreover, plasmolysis in cells occurred at the point of threshold ψ_L under drought stress conditions (Oppenheimer and Jacoby 1963). The cell volume varied correspondingly. As drought stress increased, leaf cells could no longer shrink at 80 g L^{-1} PEG level. No further considerable decrease in T_d at 80 g L^{-1} PEG level indicated that plasmolysis occurred and that the leaf cells were possibly damaged. Water status in the plants was characterized by T_d, and the variation of T_d could reflect the plant drought resistance (Wu et al. 2015). Stable T_d value at 40 g L^{-1} PEG level implied high water regulation ability of CA in the plant during drought and subsequent rewatering phases. *B. napus* exhibited good restorability at 40 g L^{-1} PEG level. These results indicated that the physiological tolerance threshold of *B. napus* to drought stress was 40 g L^{-1}.

Therefore, as a rapid non-destructive measurement parameter, T_d could be used to determine the physiological tolerance threshold of *B. napus* to drought stress and analyse its restorability under drought stress conditions. Moreover,

Table 4. Fitting equations of the relationship between leaf area (A, cm^2) and time (D, Days).

PEG concentration [g L^{-1}]	Fitting equations	R^2	*n*	*P*
0→0	$A = 19.83 + \frac{52.26}{1 + \left(\frac{D}{6.90}\right)^{-1.97}}$	0.9977	18	<0.0001
20→10	$A = 22.48 + \frac{23.57}{1 + \left(\frac{D}{4.57}\right)^{-3.57}}$	0.9930	18	<0.0001
40→20	$A = 28.52 + \frac{9.12}{1 + \left(\frac{D}{3.32}\right)^{-4.08}}$	0.9413	18	<0.0001
80→40	$A = 28.28 + \frac{-1.12^*}{1 + \left(\frac{D}{8.11}\right)^{-131.36}}$	0.5069	18	<0.0001

*Indicate that the plant ceased growing and the leaf wilted at 80→40 g L^{-1}.

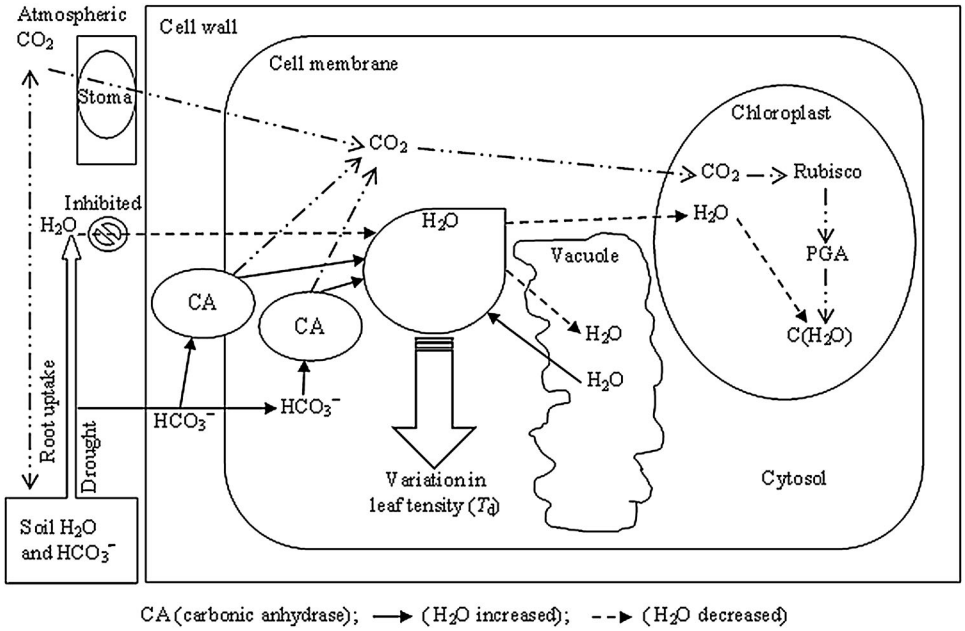

Figure 6. Movement of water in cells under drought conditions.

the prediction accuracy of physiological tolerance threshold by using T_d could be validated using the growth status of *B. napus*.

4.3. Growth status and evaluation of rewatering strategy

For many plants, leaf expansion is more sensitive to water stress than leaf abscission (Muchow 1985). The leaf is the main organ for organic matter production. Therefore, a small average leaf size will affect photosynthesis and growth. Lower transpiration can also decrease the water loss in a single plant. In some plants, having a large number of small leaves is a strategy for adapting to drought conditions (Lopez et al. 1997). However, a high leaf area growth rate comparatively offsets the photosynthetic product loss caused by leaf area decline under water stress. Therefore, the growth status of plants can be evaluated by the relative time required when the growth rate of the leaf area reaches the maximum value (RT_{GRM}). The lower the RT_{GRM} value, the faster the growth rate of the leaf area reaches the maximum value. Five rewatering strategies were set up in this study, including 80→40 g L^{-1}, 40→20 g L^{-1}, 20→10 g L^{-1} and 0→0 g L^{-1}. The rewatering strategy for *B. napus* was excellent at 40→20 g L^{-1}. Moreover, the chlorophyll content of *B. napus* at 40 g L^{-1} PEG level exhibited significantly better restorability than that at 0 g L^{-1} PEG level after rewatering. The reduction in plant dry weight at 20 and 40 g L^{-1} PEG levels was prevented compared with that at 0 g L^{-1} PEG level.

The results were consistent with the prediction of physiological tolerance threshold by using T_d.

4.4. Irrigation strategy for B. napus

Irrigation of *B. napus* was implemented at 40 g L^{-1} (−0.15 MPa) and terminated at 20 g L^{-1} (−0.11 MPa). The ψ_L values of *B. napus* at 40 and 20 g L^{-1} PEG levels were −2.20 and −0.72 MPa, respectively. According to our previous research (Hu 2016), the same ψ_L values of *B. napus* were also observed at 10.5% (P_1) and 18.4% (P_2) soil water content (P) when cultivated in loam. For example, given that the saturated soil moisture of loam (P_a) did not exceed 20%, the ratio (r) of the deficit irrigation (DI) volume to the sufficient irrigation volume (Q) of loam could be calculated as follows: $r = (P_2 - P_1/P_a - P_1)$. Therefore, V of loam was 83.2%Q. DI scheduling could be implemented on *B. napus* when cultivated in loam during the winter drought period.

5. Conclusions

Water regulation caused by enzymes, such as CA in plants, changed the variation of ψ_L and g_s, stabilized the photosynthetic capacity and delayed the water requirement in *B. napus*. T_d could reflect the plant water status better than ψ_L or g_s and played an important role in the photosynthesis of *B. napus*. No further considerable decrease in T_d at 80 g L^{-1} PEG level indicated that plasmolysis occurred and that leaf cells were possibly damaged. *B. napus* exhibited good restorability at 40 g L^{-1} PEG level. As a rapid non-destructive measurement parameter, T_d could be used to determine the physiological tolerance threshold of *B. napus* to drought stress and analyse its restorability under drought stress conditions. The results of chlorophyll content, plant dry weight and RT_{GRM} values also indicated the excellent rewatering strategy for *B. napus* at 40→20 g L^{-1}. Therefore, irrigation of *B. napus* was implemented at 40 g L^{-1} (−0.15 MPa) and terminated at 20 g L^{-1} (−0.11 MPa). Considering the same influences of drought stress on ψ_L of *B. napus*, the corresponding P values of loam were 10.5% and 18.4%, respectively. By using loam as an example, the ratio of the DI volume to the Q of loam was 83.2%. T_d could be used for the rapid determination of water requirement information in *B. napus* during winter drought period.

Disclosure statement

No potential conflict of interest was reported by the authors.

Funding

This study was supported by the project of National Natural Science Foundation of China (No. U1612441, 31301243, and 31600254); National Key Research and Development Program of China (2016YFC0502602); and Priority Academic Program Development (PAPD) of Jiangsu Higher Education Institutions.

ORCID

Deke Xing http://orcid.org/0000-0001-5834-4306

References

Batra NG, Sharma V, Kumari N. 2014. Drought-induced changes in chlorophyll fluorescence, photosynthetic pigments, and thylakoid membrane proteins of *Vigna radiata*. J Plant Interact. 9(1):712–721. doi:10.1080/17429145.2014.905801.

Bhardwaj AR, Joshi G, Kukreja B, Malik V, Arora P, Pandey R, Shukla RN, Bankar KG, Katiyar-Agarwal S, Goel S, et al. 2015. Global insights into high temperature and drought stress regulated genes by RNA-Seq in economically important oilseed crop *Brassica juncea*. BMC Plant Biol. 15(1):1–15. doi:10.1186/s12870-014-0405-1.

Dowd JE, Riggs DS. 1965. A comparison of estimates of Michaelis-Menten kinetic constants from various linear transformations. J Biol Chem. 240(2):863–869. http://www.jbc.org/content/240/2/863.citation.full.html#ref-list-1.

Fernández PA, Roleda MY, Hurd CL. 2015. Effects of ocean acidification on the photosynthetic performance, carbonic anhydrase activity and growth of the giant kelp *Macrocystis pyrifera*. Photosynth Res. 124 (3):293–304. doi:10.1007/s11120-015-0138-5.

Gallardo M, Thompson RB, Valdez LC, Fernández MD. 2006. Use of stem diameter variations to detect plant water stress in tomato. Irrigation Sci. 24(4):241–255. doi:10.1007/s00271-005-0025-5.

Gaudin R, Roux S, Tisseyre B. 2017. Linking the transpirable soil water content of a vineyard to predawn leaf water potential measurements. Agr Water Manage. 182:13–23. doi:10.1016/j.agwat.2016.12.006.

Hu LS. 2016. Water demand comparison of rape and *Orychophragmus violaceus* in the conditions of two kinds of soils. Zhenjiang: Jiangsu University. [In Chin.].

Hu HH, Boisson-Dernier A, Israelsson-Nordström M, Böhmer M, Xue SW, Ries A, Godoski J, Kuhn JM, Schroeder JI. 2011. Carbonic anhydrases are upstream regulators of CO_2-controlled stomatal movements in guard cells. Nat Cell Biol. 12(1):87–93. doi:10.1038/ncb2009.

Irigoyen JJ, Einerich DW, Sanchez-Diaz M. 1992. Water stress induced changes in concentrations of proline and total soluble sugars in nodulated alfalfa (*Medicago sativa*) plants. Physiol Plantarum. 84(1):55–60. doi:10.1111/j.1399-3054.1992.tb08764.

Kleiber T, Borowiak K, Schroeter-Zakrzewska A, Budka A, Osiecki S. 2017. Effect of ozone treatment and light colour on photosynthesis and yield of lettuce. Sci Hortic. 217:130–136. doi:10.1016/j.scienta.2017.01.035.

Kou SC, Cherayil BJ, Min W, English BP, Xie XS. 2005. Single-molecule Michaelis-Menten equations. J Phys Chem B. 109(41):19068–19081. doi:10.1021/j1490qp05.

Lopez FB, Chauhan YS, Johansen C. 1997. Effects of timing of drought stress on leaf area development and canopy light interception of short-duration pigeonpea. J Agron Crop Sci. 178(1):1–7. doi:10.1111/j.1439-037X.1997.tb00344.x.

Michel BE, Kaufmann MR. 1973. The osmotic potential of polyethylene glycol 6000. Plant Physiol. 51(5):914–916. doi:10.1104/pp.51.5.914.

Milliron LK, Olivos A, Saa S, Sanden BL, Shackel KA. 2018. Dormant stem water potential responds to laboratory manipulation of hydration as well as contrasting rainfall field conditions in deciduous tree crops. Biosyst Eng. 165:2–9. doi:10.1016/j.biosystemseng.2017.09.001.

Muchow RC. 1985. Canopy development in grain legumes grown under different soil water regimes in a semi-arid tropical environment. Field Crop Res. 11(85):99–109. doi:10.1016/0378-4290(85)90094-2.

Oppenheimer HR, Jacoby B. 1963. Does plasmolysis increase the drought tolerance of plant cells? Protoplasma. 57(1):619–627. doi:10.1007/BF01252080.

Pathan SM, Lee JD, Sleper DA, Fritschi FB, Sharp RE, CarterJr.TE, Nelson RL, King CA, Schapaugh WT, Ellersieck MR, et al. 2014. Two soybean plant introductions display slow leaf wilting and reduced yield loss under drought. J Agro Crop Sci. 200(3):231–236. doi:10.1111/jac.12053.

Porcel R, Ruiz-Lozano JM. 2004. Arbuscular mycorrhizal influence on leaf water potential, solute accumulation, and oxidative stress in soybean plants subjected to drought stress. J Exp Bot. 55(403):1743–1750. doi:10.1093/jxb/erh188.

Qaderi MM, Kurepin LV, Reid DM. 2007. Growth and physiological responses of canola (*Brassica napus*) to three components of global climate change: temperature, carbon dioxide and drought. Physiol Plantarum. 128(4):710–721. doi:10.1111/j.1399-3054.2006.00804.x.

Turner NC, Burch GJ. 1983. The role of water in plants. In: Teare ID, Peet MM, editor. Crop-water relations. New York: Wiley-Inter science; p. 73–126.

Wang SY, Su WC, Fan XR, Li C, Shi XT. 2010. Influence factors of soil moisture in karst rocky desertification region – A case study of Puding County, Guizhou Province. Res Soil Water Conserv. 17 (3):171–175. [In Chin.].

Wilbur KM, Anderson NG. 1948. Electrometric and colorimetric determination of carbonic anhydrase. J Biol Chem. 176(1):147–154.

Wu YY, Xing DK. 2012. Effect of bicarbonate treatment on photosynthetic assimilation of inorganic carbon in two plant species of Moraceae. Photosynthetica. 50(4):587–594. doi:10.1007/s11099-012-0065-z.

Wu YY, Zhang MM, Xing DK, Zhou GY. 2015. Quick reflection of moisture condition for plant using leaf tensity. Transactions of the CSAM. 46(3):310–314. [In Chin.]. doi:10.6041/j.issn.1000-1298.2015.03.045

Wu Y, Zheng XJ, Li Y. 2016. Photosynthetic response of desert plants to small rainfall events in the Junggar Basin, northwest China. Photosynthetica. 54(1):3–11. doi:10.1007/s11099-015-0168-4.

Xing DK, Wu YY. 2012. Photosynthetic response of three climber plant species to osmotic stress induced by polyethylene glycol (PEG) 6000. Acta Physiol Plant. 34(2):1659–1668. doi:10.1007/s11738-012-0961-7.

Xing DK, Wu YY, Fu WG, Li QL, Hu LS, Wu YS. 2016. Regulated deficit irrigation scheduling of *Orychophragmus violaceus based on photosynthetic physiological response traits*. Transactions of the ASABE. 59(6):1853–1860. doi:10.13031/trans.59.11853.

Zhang XD, Mao HP, Zuo ZY, Gao HY, Sun J. 2011. Nondestructive testing method for rape water stress based on multi-spectral vision. Transactions of the CSAE. 27(3):152–157. doi:10.3969/j.issn.1002-6819.2011.03.029.

Zhang MM, Wu YY, Xing DK, Zhao K, Yu R. 2015. Rapid measurement of drought resistance in plants based on electrophysiological properties. Transactions of the ASABE. 58(6):1441–1446. doi:10.13031/trans.58.11022.

Zhu SQ. 1997. Ecological research on karst forest III. Guiyang: Guizhou Science and Technology Press. [In Chin.].